Lanthanide-Based Single-Chain Nanoparticles as "Visual" Pass/Fail Sensors of Maximum Permissible Concentration of Cu2+ Ions in Drinking Water

Jokin Pinacho-olaciregui, Ester Verde-sesto, Daniel Taton, José A Pomposo

Macromolecular Rapid Communications
www.mrc-journal.de

Lanthanide-Based Single-Chain Nanoparticles as "Visual" Pass/Fail Sensors of Maximum Permissible Concentration of Cu^{2+} Ions in Drinking Water

*Jokin Pinacho-Olaciregui, Ester Verde-Sesto, Daniel Taton, and José A. Pomposo**

The maximum permissible concentration (m.p.c.) of Cu^{2+} ions in drinking water, as set by the World Health Organization (WHO) is m.p.c. $(Cu^{2+})_{WHO} = 30 \times 10^{-6}$ M, whereas the US Environmental Protection Agency (EPA) establishes a more restrictive value of m.p.c. $(Cu^{2+})_{EPA} = 20 \times 10^{-6}$ M. Herein, for the first time ever, a family of m.p.c. (Cu^{2+}) "visual" pass/fail sensors is developed based on water-soluble lanthanide-containing single-chain nanoparticles (SCNPs) exhibiting an average hydrodynamic diameter less than 10 nm. Both europium (Eu)- and terbium (Tb)-based SCNPs allow excessive Cu^{2+} to be readily detected in water, as indicated by the red-to-transparent and green-to-transparent changes, respectively, under UV light irradiation, occurring at 30×10^{-6} M Cu^{2+} in both cases. Complementary, dysprosium (Dy)-based SCNPs show a yellow color-to-transparent transition under UV light irradiation at $\approx 15 \times 10^{-6}$ M Cu^{2+}. Eu-, Tb-, and Dy-containing SCNPs prove to be selective for Cu^{2+} ions as they do not respond against other metal ions, such as Fe^{2+}, Ag^{+}, Co^{2+}, Ba^{2+}, Ni^{2+}, Hg^{2+}, Pb^{2+}, Zn^{2+}, Fe^{3+}, Ca^{2+}, Mn^{2+}, Mg^{2+}, or Cr^{3+}. These new m.p.c. (Cu^{2+}) "visual" pass/fail sensors are thoroughly characterized by a combination of techniques, including size exclusion chromatography, dynamic light scattering, inductively coupled plasma-mass spectrometry, as well as infrared, UV, and fluorescence spectroscopy.

1. Introduction

Copper is an essential trace element for animals and plants.[1] In fact, Cu^{2+} – the 3th most important metal ion present in biological system – is involved as cofactor of numerous metalloenzymes.[2,3] Cu^{2+} ions are also essential for the human body and defect of this crucial micronutrient can impart cytopenia (a reduction in the number of mature blood cells) and profound neurological deficits.[4,5] On the contrary, an excessive Cu^{2+} intake from occupational exposure or contaminated water can cause gastrointestinal problems, liver and kidney damage, hemolytic anemia and impaired immune function, among other effects.[6,7] Thus, Cu^{2+} ions act as one of the environment pollutants to control due to their increased use at several levels (home, industrial, and agricultural operations), as well as environmental persistency.[8]

Different regulatory Organisms have established the maximum permissible concentration (m.p.c.) of Cu^{2+} ions in drinking water. The m.p.c. of Cu^{2+} ions in drinking water by the World Health Organization (WHO) is m.p.c. $(Cu^{2+})_{WHO} = 30 \times 10^{-6}$ M, whereas the US Environmental Protection Agency (EPA) establishes a more restrictive value of m.p.c. $(Cu^{2+})_{EPA} = 20 \times 10^{-6}$ M.[9,10] Although different analytical techniques are available to accurately determine the concentration of Cu^{2+} ions in drinking water (e.g., atomic absorption spectroscopy, ion chromatography, inductively coupled plasma mass spectrometry), these techniques often involve sophisticated instrumentation

J. Pinacho-Olaciregui, E. Verde-Sesto, J. A. Pomposo
Centro de Física de Materiales (CSIC – UPV/EHU) – Materials Physics Center MPC
Paseo Manuel Lardizabal 5, Donostia E-20018, Spain
E-mail: Josetxo.pomposo@ehu.eus

The ORCID identification number(s) for the author(s) of this article can be found under https://doi.org/10.1002/marc.202400116

DOI: 10.1002/marc.202400116

J. Pinacho-Olaciregui, D. Taton
Laboratoire de Chimie des Polymères Organiques (LCPO)
Université de Bordeaux INP-ENSCBP
16 av. Pey Berland, Pessac cedex 33607, France

E. Verde-Sesto, J. A. Pomposo
IKERBASQUE – Basque Foundation for Science
Plaza Euskadi 5, Bilbao E-48009, Spain

J. A. Pomposo
Departamento de Polímeros y Materiales Avanzados: Física Química y Tecnología University of the Basque Country (UPV/EHU)
Paseo Manuel Lardizabal 3, Donostia E-20800, Spain

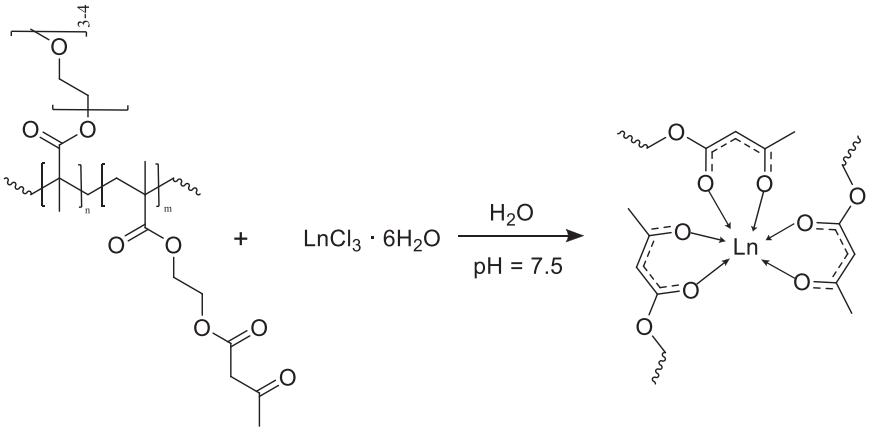

Scheme 1. Schematic illustration of the synthesis of lanthanide (Ln)-based single-chain polymer nanoparticles (SCNPs) using an amphiphilic random copolymer decorated with *beta*-ketoester functional groups, namely, poly(OEGMA-*co*-AEMA) (see text).

and require skilled users. Consequently, alternative methods based on "visual" pass/fail sensors providing operational simplicity, sensitivity, and selectivity are highly desirable. To tackle that challenge, we envisioned to design single-chain polymer nanoparticles (SCNPs) incorporating lanthanide metal ions as a versatile platform towards a new generation of m.p.c. (Cu^{2+}) "visual" pass/fail sensors. SCNPs are individual polymeric chains intramolecularly folded through intrachain interactions.[11] The folding of discrete synthetic polymer chains into SCNPs attempts to mimic the natural folding of biomacromolecules, such as proteins.[12] The chain folding process leads to locally compact domains within SCNPs, which can be of practical use to bind active species (e.g., metal ions,[13] luminophores,[14] drugs.[15]). Consequently, SCNPs offer interesting opportunities for the development of improved sensors,[16] innovative drug delivery vehicles,[17] and biomimetic catalysts,[18] including bimetallic Eu(III)/Pt(II)-SCNPs with both luminescent properties and catalytic activity.[19] On the other hand, a variety of complexes based on lanthanide ions.[20–23] have been investigated as fluorescent "turn-off" sensors of Cu^{2+} ions. However, most of these molecular sensors are not directly operative in water, but instead, in organic solvent/water mixtures.

We hypothesized that, by using an amphiphilic random copolymer featuring *beta*-ketoester functional groups able to complex with lanthanide ions, water-soluble lanthanide-containing SCNPs could be achieved via intrachain *beta*-ketoester/ lanthanide complexation. The resulting lanthanide-based SCNPs were thus employed as innovative m.p.c. (Cu^{2+}) "visual" pass/fail sensors in drinking water. Here we report the synthesis of europium (Eu)-, terbium (Tb)-, and dysprosium (Dy)-based SCNPs, as well as their use—for the first time ever—as efficient "visual" pass/fail sensors of maximum permissible concentration of Cu^{2+} ions in water.

2. Results and Discussion

2.1. Eu-SCNPs as m.p.c. (Cu^{2+}) "Visual" Pass/Fail Sensors

Europium-based single-chain nanoparticles (Eu-SCNPs) were prepared at a concentration of 1 mg mL^{-1}, following the procedure depicted in **Scheme 1**. A linear amphiphilic random copolymer, namely, poly(OEGMA-*co*-AEMA) was first synthesized by RAFT copolymerization of the hydrophilic monomer OEGMA and the hydrophobic monomer AEMA. Poly(OEGMA-*co*-AEMA) was found to contain 35 mol% of *beta*-ketoester functional groups, as determined by ^{1}H NMR spectroscopy (see Figure S1 in the Supporting Information). Poly(OEGMA-*co*-AEMA) showed a weight-average molecular weight of M_w = 80.7 kDa and relatively low dispersity, $Đ$ = 1.11 (Table S1, Supporting Information). Eu-SCNPs resulted from the complexation of Eu^{3+} ions in solution by *beta*-ketoester functional groups of poly(OEGMA-*co*-AEMA) (see Scheme 1). The formation of Ln^{3+}/*beta*-ketoester complexes involving low molecular weight organic compounds is well documented.[24–26] To the best of our knowledge, however, there are no precedents of single-chain polymer nanoparticle formation via intrachain lanthanide/*beta*-ketoester complex formation. Successful preparation of Eu-SCNPs was confirmed by a combination of structural and size characterization techniques. Hence, SEC results confirmed a shift of the SEC elution time at peak maximum towards longer retention time and, hence, smaller hydrodynamic size for Eu-SCNPs when compared to the parent poly(OEGMA-*co*-AEMA) (see **Figure 1a**). Eu-SCNPs showed M_w = 85.0 kDa and $Đ$ = 1.12, suggesting the folding of individual copolymer chains and the absence of multichain aggregates by intermolecular crosslinking.[11] Complementary, DLS measurements showed a decrease of the average hydrodynamic diameter from 8.3 to 7.3 nm upon formation of Eu-SCNPs via intrachain Eu^{3+}/*beta*-ketoester complexation (see Figure S2 in the Supporting Information). The Eu-SCNPs were found to exhibit fluorescent properties under UV irradiation (λ_{exc} = 254 nm), in a range of pH between 7.5 and 11 (see Figure 1b; Figures S3–S5, Supporting Information) even if the precursor Eu(III) salt was not fluorescent in water. Thus, at low pH value the Ln/*beta*-ketoester interactions were disrupted, whereas high pH caused the aggregation of the Eu-SCNPs, which ultimately led to their macroscopic precipitation from the solution. FTIR spectroscopy provided further evidence of the presence of Eu^{3+}/*beta*-ketoester complexes in Eu-SCNPs. As illustrated in Figure 1c, an intense band located at 1632.4 cm^{-1} indeed appeared in the FTIR spectrum of the

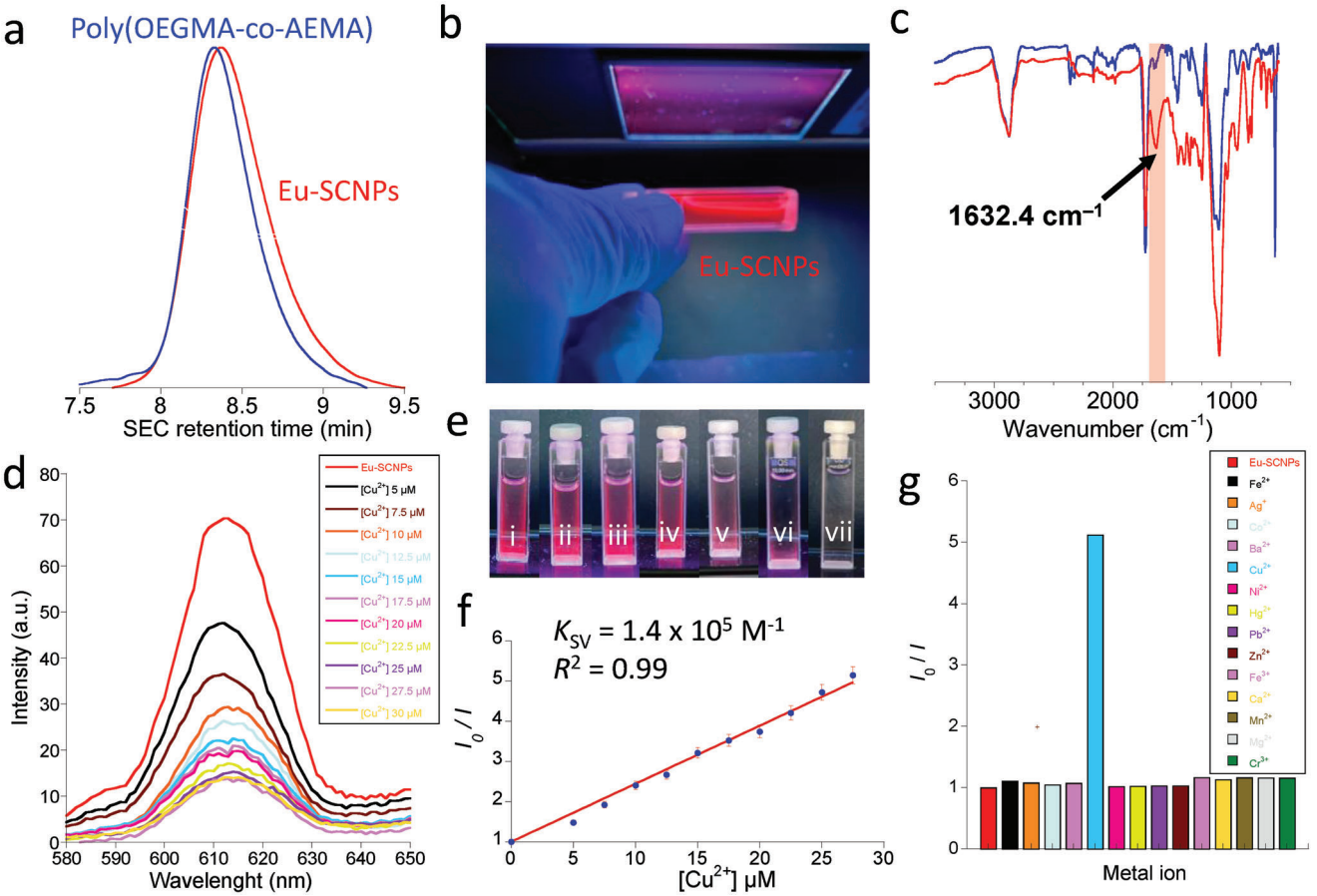

Figure 1. Europium-based single-chain nanoparticles (Eu-SCNPs) as "visual" pass/fail sensors of maximum permissible concentration (m.p.c.) of Cu^{2+} ions in water: a) SEC traces of the precursor, poly(OEGMA-*co*-AEMA), and the Eu-SCNPs, b) illustration of the reddish fluorescent Eu-SCNPs under UV light irradiation (λ_{exc} = 254 nm), c) FTIR spectra of poly(OEGMA-*co*-AEMA) (blue color) and Eu-SCNPs (red color), d) PL spectra of Eu-SCNPs in water in the presence of increasing amounts of Cu^{2+} ions, e) demonstration of the utility of Eu-SCNPs as "visual" pass/fail sensors of m.p.c. of Cu^{2+} ions in water according to the WHO criterion ((i): 5×10^{-6} M, (ii): 10×10^{-6} M, (iii): 15×10^{-6} M, (iv): 22.5×10^{-6} M, (v): 25×10^{-6} M, (vi): 27.5×10^{-6} M, and (vii): 30×10^{-6} M), f) Stern–Volmer plot ($I_0 / I = 1 + K_{SV}[Cu^{2+}]$) of Eu-SCNPs (error bars estimated from triple measurements) and g) selectivity of Eu-SCNPs for Cu^{2+} ions against other metal ions.

Eu-SCNPs, which could be assigned to the stretching vibration of the enol tautomer of the beta-ketoester groups bonded to Eu^{3+}. Figure 1d shows the PL spectra of Eu-SCNPs in water in the presence of increasing amounts of Cu^{2+} ions (λ_{exc} = 254 nm). As shown in Figure 1e, Eu-SCNPs can be used as "visual" pass/fail sensors of m.p.c. of Cu^{2+} ions in water, according to the WHO criterion (m.p.c. $(Cu^{2+})_{WHO} = 30 \times 10^{-6}$ M).[9] A clear red color-to-transparent change under UV light (λ_{exc} = 254 nm) is indeed observed in Figure 1e on passing from $[Cu^{2+}] \leq 27.5 \times 10^{-6}$ M to $[Cu^{2+}] = 30 \times 10^{-6}$ M (or above, data not shown). Analysis of the data in Figure 1d using the Stern–Volmer equation.[27] ($I_0 / I = 1 + K_{SV}[Cu^{2+}]$) provided a value of $K_{SV} = 1.4 \times 10^5$ M^{-1} and a squared coefficient of linear regression of $R^2 = 0.99$ (see Figure 1f). Remarkably, Eu-SCNPs proved highly selective for Cu^{2+} ions against other metal ions, such as Fe^{2+}, Ag^{+}, Co^{2+}, Ba^{2+}, Ni^{2+}, Hg^{2+}, Pb^{2+}, Zn^{2+}, Fe^{2+}, Ca^{2+}, Mn^{2+}, Mg^{2+}, and Cr^{3+} (Figure 1g). Eu^{3+} emission quenching is due to energy transfer to Cu^{2+} and, then, nonradiative relaxation to the ground state of Cu^{2+}.[28,29] Additional characterization data of the Eu-SCNPs can be found in the Supporting Information (Figures S6–S8, Supporting Information).

2.2. Tb-SCNPs as m.p.c. (Cu^{2+}) "Visual" Pass/Fail Sensors

Tb-SCNPs were obtained from the complexation of Tb^{3+} ions in solution by *beta*-ketoester functional groups of poly(OEGMA-*co*-AEMA), as displayed in Scheme 1. The average hydrodynamic diameter of the Tb-SCNPs was 7.2 nm (**Figure 2a**), a value smaller than that of the poly(OEGMA-*co*-AEMA) precursor (8.3 nm). The SEC trace of Tb-SCNPs (M_w = 88.9 kDa, $Đ$ = 1.36, see Table S1 in the Supporting Information) confirmed the absence of multi-chain aggregates, in accordance with DLS results shown in Figure 2a. The Tb-based SCNPs were visualized as greenish fluorescent nanomaterials under UV light irradiation (λ_{exc} = 254 nm) in a range of pH between 7.5 and 9 (see Figure 2b; Figures S9–S11, Supporting Information). Under strong acidic conditions the fluorescence disappeared due to the disruption

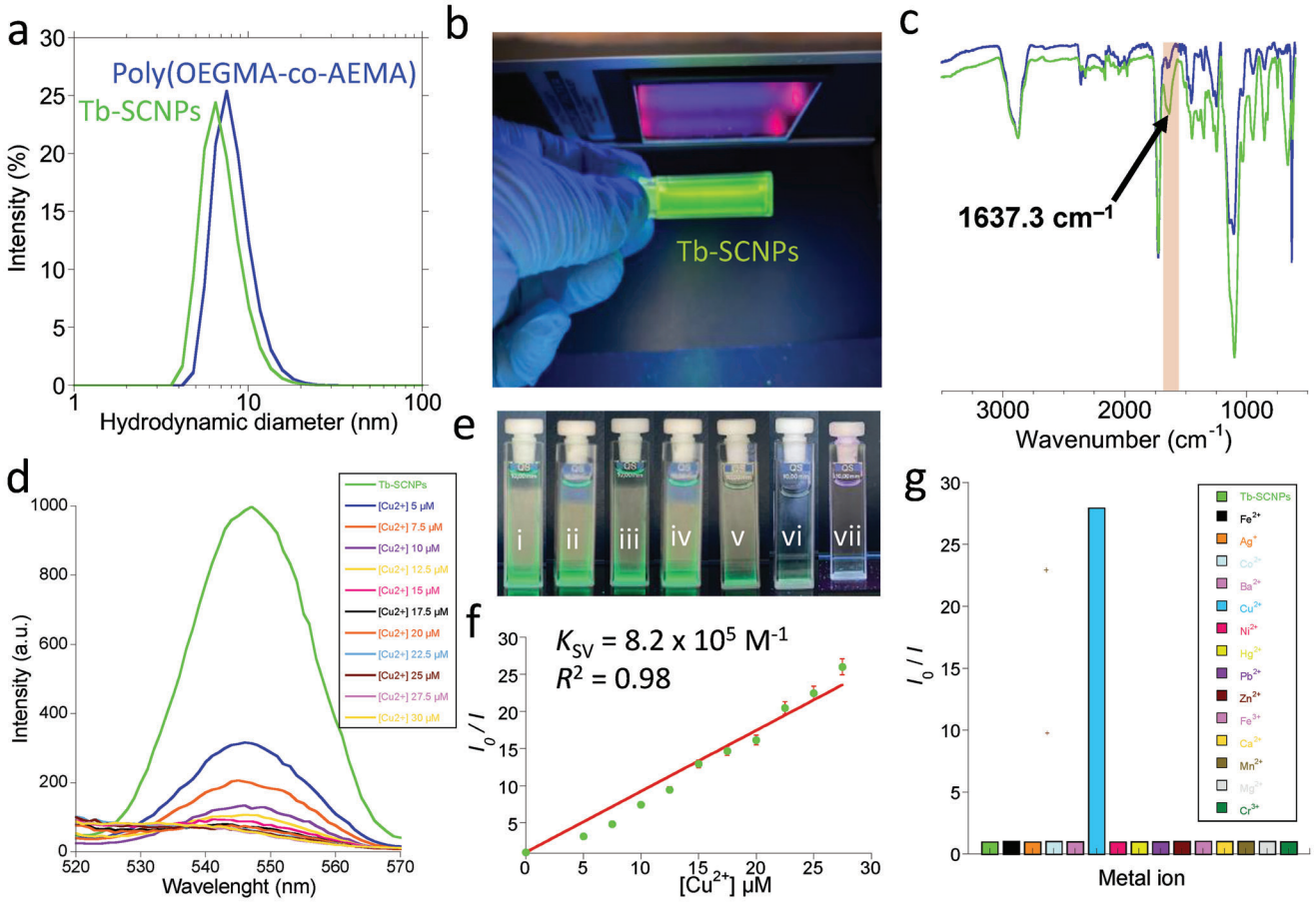

Figure 2. Terbium-based single-chain polymer nanoparticles (Tb-SCNPs) as "visual" pass/fail sensors of maximum permissible concentration (m.p.c.) of Cu^{2+} ions in water: a) DLS size distribution of the precursor, poly(OEGMA-*co*-AEMA), and the Tb-SCNPs, b) illustration of the greenish fluorescent Tb-SCNPs under UV light irradiation (λ_{exc} = 254 nm), c) FTIR spectra of poly(OEGMA-*co*-AEMA) (blue color) and Tb-SCNPs (green color), d) PL spectra of Tb-SCNPs in water in the presence of increasing amounts of Cu^{2+} ions, e) demonstration of the utility of Tb-SCNPs as "visual" pass/fail sensors of m.p.c. of Cu^{2+} ions in water according to the WHO criterion ((i): 2.5×10^{-6} M, (ii): 5×10^{-6} M, (iii): 15×10^{-6} M, (iv): 22.5×10^{-6} M, (v): 25×10^{-6} M, (vi): 27.5×10^{-6} M, and (vii): 30×10^{-6} M), f) Stern–Volmer plot of Tb-SCNPs (error bars estimated from triple measurements), and g) selectivity of Tb-SCNPs for Cu^{2+} ions against other metal ions.

of Tb^{3+}/*beta*-ketoester complexes, whereas under high basic pH a decrease in fluorescence was noted, as a consequence of aggregation of the Tb-SCNPs. The stretching vibration of the enol tautomer of the *beta*-ketoester groups bonded to Tb^{3+} was observed at 1637.3 cm^{-1} in the FTIR spectrum of Tb-SCNPs (Figure 2c). PL spectra of Tb-SCNPs in water in the presence of increasing amounts of Cu^{2+} ions (λ_{exc} = 254 nm) are given in Figure 2d. A clear green color-to-transparent change under UV light (λ_{exc} = 254 nm) was thus observed by the naked-eye, on passing from $[Cu^{2+}] \leq 27.5 \times 10^{-6}$ M to $[Cu^{2+}] = 30 \times 10^{-6}$ M or above (Figure 2e). In other words, Tb-SCNPs proved very useful as "visual" pass/fail sensors of m.p.c. of Cu^{2+} ions in water, according to the WHO criterion (m.p.c. $(Cu^{2+})_{WHO} = 30 \times 10^{-6}$ M).[9] Analysis of the data in Figure 2d using the Stern–Volmer equation provided $K_{SV} = 8.2 \times 10^5$ M^{-1} and $R^2 = 0.98$ (see Figure 2f). The higher value of K_{SV} for Tb-SCNPs relatively to Eu-SCNPs indicates a strong sensing ability of Tb-SCNPs when compared to Eu-SCNPs. Moreover, Tb-based SCNPs display high selectivity for Cu^{2+} ions against a variety of other metal ions (Figure 2g). Additional data of Tb-SCNPs are available in the Supporting Information (Figures S12–S14, Supporting Information).

2.3. Dy-SCNPs as m.p.c. (Cu^{2+}) "Visual" Pass/Fail Sensors

Dy-SCNPs synthesized via complexation of Dy^{3+} ions in solution by *beta*-ketoester functional groups of poly(OEGMA-*co*-AEMA) showed an average hydrodynamic diameter of 7.6 nm, a value smaller than that of the poly(OEGMA-*co*-AEMA) precursor (**Figure 3a**). Dy-SCNPs displayed yellowish fluorescence under UV light irradiation (λ_{exc} = 254 nm) in a pH range between 7.5 and 9. Similar to the case of Eu-SCNPs and Tb-SCNPs, the fluorescence of Dy-based SCNPs could be switched-off at very low pH, owing to rupture of Dy^{3+}/*beta*-ketoester complexes or high pH (because of the appearance of aggregation and precipitation phenomena). Dy-based SCNPs were found to display yellowish fluorescence by the naked eye under UV light irradiation at λ_{exc} = 254 nm (Figure 3b). In the FTIR spectrum of the Dy-based

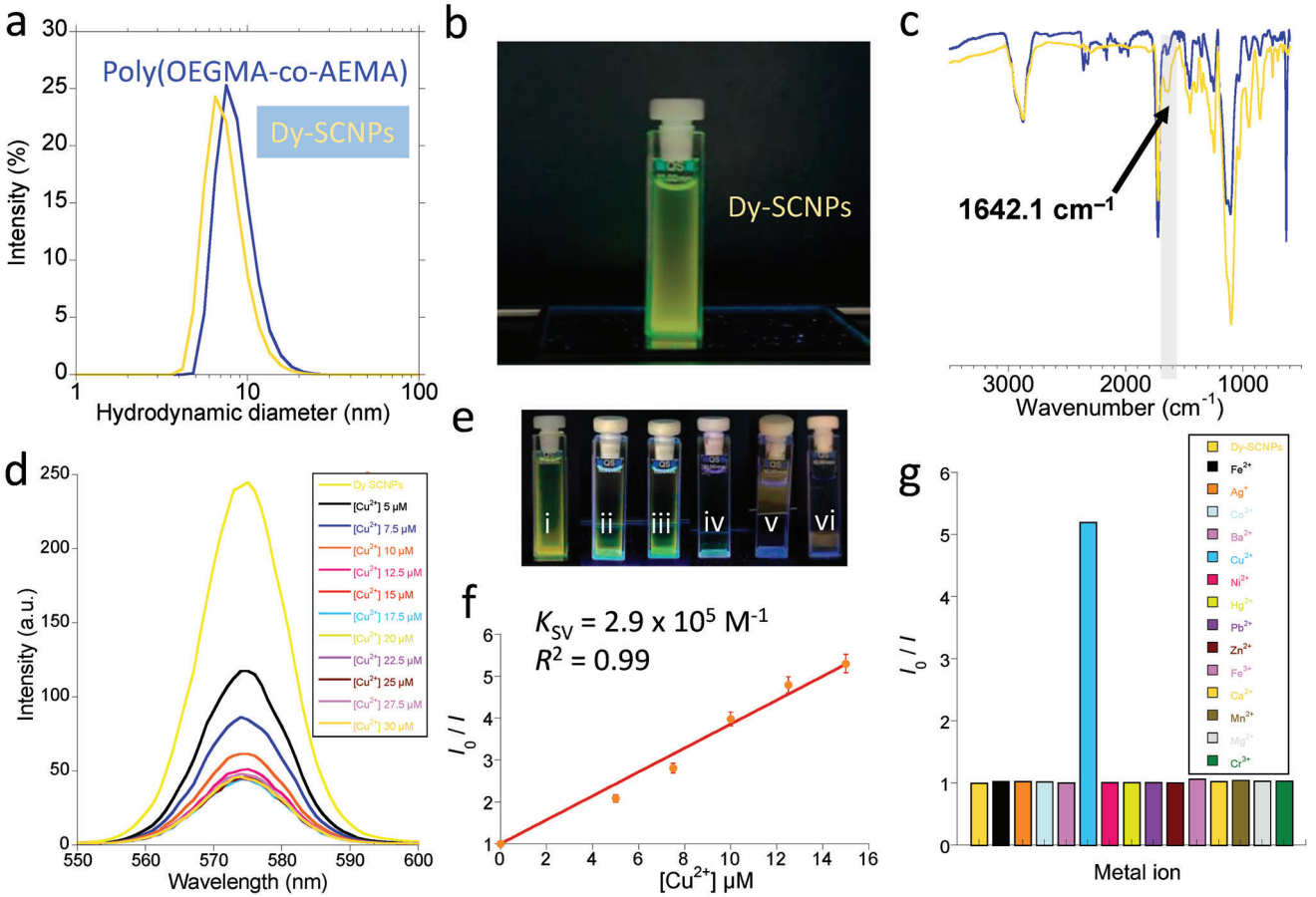

Figure 3. Dysprosium-based single-chain polymer nanoparticles (Dy-SCNPs) as "visual" pass/fail sensors of maximum permissible concentration (m.p.c.) of Cu^{2+} ions in water: a) DLS size distribution of the precursor, poly(OEGMA-*co*-AEMA), and the Dy-SCNPs, b) illustration of the yellowish fluorescent Dy-SCNPs under UV light irradiation (λ_{exc} = 254 nm), c) FTIR spectra of poly(OEGMA-*co*-AEMA) (blue color) and Dy-SCNPs (green color), d) PL spectra of Dy-SCNPs in water in the presence of increasing amounts of Cu^{2+} ions, e) demonstration of the utility of Dy-SCNPs as "visual" pass/fail sensors of m.p.c. of Cu^{2+} ions in water according to the EPA criterion ((i): 1×10^{-6} M, (ii): 2.5×10^{-6} M, (iii): 10×10^{-6} M, (iv): 15×10^{-6} M, (v): 20×10^{-6} M, and (vi): 30×10^{-6} M), f) Stern–Volmer plot of Dy-SCNPs (error bars estimated from triple measurements), and g) selectivity of Dy-SCNPs for Cu^{2+} ions against other metal ions.

SCNPs, the stretching vibration of the enol tautomer of the beta-ketoester groups bonded to Dy^{3+} was observed at 1642.1 cm^{-1} (Figure 3c). Interestingly, Dy-SCNPs show a yellow color-to-transparent transition under UV light irradiation at ≈15×10^{-6} M of Cu^{2+} ions (Figure 3d,e) – very close to the US-EPA criterion (m.p.c. $(Cu^{2+})_{EPA} = 20 \times 10^{-6}$ M) – making these Dy-based SCNPs practical "visual" pass/fail sensors of m.p.c. of Cu^{2+} ions in water according to the EPA regulation. A Stern–Volmer plot for Dy-SCNPs provided $K_{SV} = 2.9 \times 10^5$ M^{-1} and $R^2 = 0.99$ (see Figure 3f). Similarly to Eu-based and Tb-based SCNPs, Dy-based SCNPs proved selective for Cu^{2+} ions against other metal ions in solution. Additional data of Dy-SCNPs are available in the Supporting Information (Figures S15–S19, Supporting Information).

3. Conclusion

We introduced a new generation of m.p.c. (Cu^{2+}) "visual" pass/fail sensors based on water-soluble lanthanide (Eu, Tb, or Dy)-containing SCNPs of sub-10 nm size range. Under UV light irradiation at λ_{exc} = 254 nm, Eu-SCNPs and Tb-SCNPs showed naked-eye red color-to-transparent and green color-to-transparent transitions, respectively, near $[Cu^{2+}] = 30 \times 10^{-6}$ M in water at pH = 7.5. As for Dy-based SCNPs, they displayed a yellow color-to-transparent transition at approximately $[Cu^{2+}] = 15 \times 10^{-6}$ M. The characteristic FTIR stretching vibration of the enol tautomer of the *beta*-ketoester groups bonded to Eu^{3+}, Tb^{3+}, and Dy^{3+} ions in Eu-SCNPs, Tb-SCNPs, and Dy-SCNPs was located at 1632.4, 1637.3, and 1642.1 cm^{-1}, respectively. These "visual" pass/fail sensors show high selectivity towards Cu^{2+} ions against a variety of other metal ions (Fe^{2+}, Ag^{+}, Co^{2+}, Ba^{2+}, Ni^{2+}, Hg^{2+}, Pb^{2+}, Zn^{2+}, Fe^{2+}, Ca^{2+}, Mn^{2+}, Mg^{2+}, and Cr^{3+}). Consequently, Eu-SCNPs and Tb-SCNPs can be used as "visual" pass/fail sensors of m.p.c. of Cu^{2+} ions in water according to the WHO criterion (m.p.c. $(Cu^{2+})_{WHO} = 30 \times 10^{-6}$ M). Complementary, Dy-SCNPs can be useful as "visual" pass/fail sensors of m.p.c. of Cu^{2+} ions in water according to the EPA regulation (m.p.c. $(Cu^{2+})_{EPA} = 20 \times 10^{-6}$ M).

4. Experimental Section

Materials: Oligo(ethylene glycol) methyl ether methacrylate (OEGMA) (average $M_n \approx 300$ g mol^{-1}), (2-acetoacetoxy)ethyl methacrylate (AEMA) (95%), 2,2-azobis(2-methylpropionitrile) (AIBN) (≥98%), triethylamine (Et3N) (>99%), methyl acetoacetate 99%, 1,4-dioxane (anhydrous, 99.8%), *n*-hexane (anhydrous, 95%), 4-cyano-4-(thiobenzoylthio)pentanoic acid (≥ 97%), europium trichloride hexahydrate ($EuCl_3$•6 H_2O) (99.99% trace metals basis), terbium trichloride hexahydrate ($TbCl_3$•6 H_2O) (99.99% trace metals basis), dysprosium trichloride hexahydrate ($DyCl_3$•6 H_2O) (99.99% trace metals basis), copper (II) acetate (98%), iron (II) acetate (95%), cobalt (II) acetate tetrahydrate (99%), barium acetate (99%), nickel (II) acetate tetrahydrate (99%), mercury (II) acetate (≥ 98.0%), lead (II) acetate tetrahydrate (99%) zinc (II) acetate dehydrate (99%), iron (III) acetylacetonate (97%), calcium acetate monohydrate (99%), manganese (II) acetylacetone (98%), magnesium chloride (98%), and chromium(III) acetate (98%) were supplied by Merk (Sigma-Aldrich). Potassium hydroxide (KOH) (≥ 85%, pellets) was supplied by PanReac AppliChem (ITW Reagents). Silver (I) acetate (99%) was supplied by ITW Reagents (Acros Organics). Deionized water was obtained from a Thermo Scientific apparatus (Barnstead TII Pure Water System). Tetrahydrofuran (THF) was supplied by Scharlab. Deuterated chloroform ($CDCl_3$) (99.8 atom % D) was supplied by Merk.

Techniques: ^{1}H nuclear magnetic resonance (NMR) spectra were obtained at room temperature (r.t.) using a Bruker spectrometer operating at 400 MHz with $CDCl_3$ as the solvent. Size exclusion chromatography (SEC) measurements were conducted at 30 °C in an Agilent 1200 system that was equipped with PLgel 5 µm Guard and PLgel 5 µm MIXED-C columns. The measurements employed a triple detection system, which included a differential refractive index detector (Optilab Rex, Wyatt), a multi-angle laser light scattering (MALLS) detector (MiniDawn Treos, Wyatt), and a viscosimetric (VIS) detector (ViscoStar-II, Wyatt). SEC data were analyzed using Wyatt's ASTRA Software (version 6.1). Tetrahydrofuran (THF) was used as the eluent with a flow rate of 1 mL min^{-1}. For both the precursor and the single-chain nanoparticles, a value of $dn/dc = 0.1150$ was applied. Dynamic light scattering (DLS) measurements were carried out at r.t. on a Malvern Zetasizer Nano ZS apparatus. Metal content in the single-chain nanoparticles was determined by inductively coupled plasma mass spectrometry (ICP-MS). Fourier transform infrared (FTIR) spectra were recorded at r.t. on a JASCO 3600 FTIR spectrometer. UV spectroscopy was carried out in an Agilent 8453A spectrometer. Photoluminescence (PL) spectra were recorded at r.t. on an Agilent Cary Eclipse spectrometer. Horiba Laquatwin-pH-33 compact pH-meter was used for pH measurements.

Methods—Synthesis of Amphiphilic Random Copolymer Featuring Beta-Ketoester Functional Groups: OEGMA (1.54 mL, 5.6 mmol), AEMA (0.26 mL, 1.38 mmol), 4-cyano-4-(thiobenzoylthio)pentanoic acid (18.3 mg, 0.065 mmol), and AIBN (2.15 mg, 0.013 mmol) were dissolved at r.t. in 1,4-dioxane (3 mL). The resulting mixture was degassed by purging with argon for 15 min. Then, the mixture was subjected to reversible addition fragmentation chain-transfer (RAFT) copolymerization at 70 °C for 24 h. The resulting poly(OEGMA-*co*-AEMA) copolymer, a pink oil, was isolated by precipitation in hexane. Subsequently, the product was dissolved in a minimal amount of THF and added to an excess of hexane (twice). After removal of volatile organic solvents, further drying was carried out at r.t. under vacuum.

Synthesis of Lanthanide-Based Single-Chain Polymer Nanoparticles (SCNPs): Poly(OEGMA-*co*-AEMA) (15 mg, 0.03 mmol) and the corresponding lanthanide trichloride hexahydrate ($LnCl_3$•6 H2O; Ln = Eu, Tb, Dy) (30×10^{-6} M) were dissolved in water (15 mL) at r.t. and pH = 7.5 for 24 h. The resulting lanthanide-containing SCNPs were purified by dialysis against deionized water. ICP-MS data about the lanthanide content in the SCNPs are provided in the ESI. Successful formation of SCNPs was confirmed by SEC and DLS measurements, according to well-established literature procedures.[11] To mitigate possible interference from molecular oxygen, all lanthanide-based SCNPs were subjected to an extensive degassing (N_2) process before performing the fluorescence measurements.

Supporting Information

Supporting Information is available from the Wiley Online Library or from the author.

Acknowledgements

The authors gratefully acknowledge Grant PID2021-123438NB-I00 funded by MCIN/AEI/10.13039/501100011033 and "ERDF A way of making Europe", Grant TED2021-130107A-I00 funded by MCIN/AEI/10.13039/501100011033 and Unión Europea "NextGenerationEU/PRTR" and Grant IT-1566-22 from Eusko Jaurlaritza (Basque Government). J. P.-O. acknowledges a predoctoral contract for the completion of his Ph.D. thesis under a joint supervision between University of the Basque Country (UPV/EHU) and University of Bordeaux (UB). The authors thank for technical and human support provided by SGIker of UPV/EHU.

Conflict of Interest

The authors declare no conflict of interest.

Data Availability Statement

The data that support the findings of this study are available from the corresponding author upon reasonable request.

Keywords

environmental sensors, Cu^{2+} ions, lanthanide complexes, single-chain nanoparticles (SCNPs)

Received: February 27, 2024
Revised: March 22, 2024
Published online:

[1] R. A. Muttkowski, *Science* **1921**, *53*, 453.
[2] W. Kaim, J. Rall, *Angew. Chem., Int. Ed.* **1996**, *35*, 43.
[3] B. E. Kim, T. Nevitt, D. J. Thiele, *Nat. Chem. Biol.* **2008**, *4*, 176.
[4] T. R. Halfdanarson, N. Kumar, C. Y. Li, R. L. Phyliky, W. J. Hogan, *Eur. J. Haematol.* **2008**, *80*, 523.
[5] M. C. Linder, *Int. J. Mol. Sci.* **2020**, *21*, 4932
[6] F. Pizarro, M. Olivares, R. Uauy, Contreras, P. C, A. Rebelo, V. Gidi, *Environ. Health Perspect.* **1999**, *107*, 117.
[7] G. Brewer, *Clin. Neurophysiol.* **2010**, *121*, 459.
[8] P. G. Georgopoulos, A. Roy, M. J. Yonone-Lioy, R. E. Opiekun, P. J. Lioy, *J. Toxicol. Environ. Health B Crit. Rev.* **2001**, *4*, 341.
[9] Copper in Drinking-water, World Health Organization (WHO), **2004**.
[10] Copper Facts, US Environmental Protection Agency (EPA), **2008**.
[11] *Single-Chain Polymer Nanoparticles: Synthesis, Characterization, Simulations and Applications* (Ed. J. A. Pomposo), Wiley-VCH, Weinheim **2017**.
[12] A. Latorre-Sánchez, J. A. Pomposo, *Polym. Int.* **2016**, *65*, 855.
[13] M. A. J. Gillissen, I. K. Voets, E. W. Meijer, A. R. A. Palmans, *Polym. Chem.* **2012**, *3*, 3166.
[14] J. De-La-Cuesta, E. Verde-Sesto, A. Arbe, J. A. Pomposo, *Angew. Chem., Int. Ed.* **2021**, *60*, 3534.
[15] C. C. Cheng, D. J. Lee, Z. S. Liao, J. J. Huang, *Polym. Chem.* **2016**, *7*, 6164.

[16] A. Latorre-Sánchez, J. A. Pomposo, *Chem. Commun.* **2015**, *51*, 15736.
[17] N. M. Hamelmann, J. W. D. Paats, Y. Avalos-Padilla, E. Lantero, I. Siden-Kiamos, L. Spanos, X. Fernandez-Busquets, J. M. J. Paulusse, *ACS Infect. Dis.* **2023**, *9*, 56.
[18] S. Garmendia, S. B. Lawrenson, M. C. Arno, R. K. O'Reilly, D. Taton, A. P. Dove, *Macromol. Rapid Commun.* **2019**, *40*, 1900071.
[19] N. D. Knöfel, H. Rothfuss, P. Tzvetkova, B. Kulendran, C. Barner-Kowollik, P. W. Roesky, *Chem. Sci.* **2020**, *11*, 10331.
[20] T. Gunnlaugsson, J. P. Leonard, K. Sénéchal, A. J. Harte, *Chem. Commun.* **2004**, 782.
[21] A. Nonat, A. J. Harte, K. Senechal-David, J. P. Leonard, T. Gunnlaugsson, *Dalton Trans.* **2009**, 4703.
[22] Z. Ekmekci, *Tetrahedron Lett.* **2015**, *56*, 1878.
[23] L. M. Aroua, R. Ali, A. E. A. E. Albadri, S. Messaoudi, F. M. Alminderej, S. M. Saleh, *Biosensors* **2023**, *13*, 359.
[24] B. S. Sankha, R. N. Kapoor, *Can. J. Chem.* **1966**, *44*, 1369.
[25] N. K. Dutt, S. Rahut, *J. Inorg. Nucl. Chem.* **1969**, *31*, 3177.
[26] A. M. Mishchenko, E. K. Trunova, A. S. Berezhnytska, *J. Solution Chem.* **2015**, *44*, 2117.
[27] O. Stern, M. Volmer, *Z. Phys.* **1919**, *20*, 183.
[28] M. L. Aulsebrook, B. Graham, M. R. Grace, K. L. Tuck, *Coord. Chem. Rev.* **2018**, *375*, 191.
[29] K. Szyszka, S. Targońska, A. Lewińska, A. Watras, R. J. Wiglusz, *Nanomaterials* **2021**, *11*, 464.